

Online Supplementary Material for:

Wyoming on the run – toward final Paleoproterozoic assembly of Laurentia

*Taylor M. Kilian, Kevin R. Chamberlain, David A.D. Evans, Wouter Bleeker,
and Brian L. Cousens*

This file contains:

Supplementary text

Supplementary figures (Figs. DR(1–9))

Supplementary tables (Tables DR(1–5))

Supplementary references

SUPPLEMENTARY TEXT

Sourdough Dikes

When viewed on a large scale (Fig. DR1), the Sourdough dikes appear small in number and distributed nearly along strike of each other. With respect to paleomagnetic data, this raises concerns about sampling the same cooling units multiple times, thereby leading to falsely averaged secular variation. There are a few large Sourdough dikes (three over 10 m wide), but the majority are small intrusions that extend for only hundreds of meters (eight dikes are under 2.5 m wide). This is especially important in the Beartooth Mountains (near Glacier Lake) where a series of intrusions crop out nearly along strike of each other (sites BT22, BT23, BT42, and BT43), yet are clearly separate cooling units with visible extents (Fig. DR2). Many small dikes also occur in the central Bighorn Mountains (Fig. DR3) parallel to each other (BH61-63) and slightly offset along strike. In both cases, the extent of dikes are clear enough to distinguish them as separate

cooling units, except in the case of BH50 and BH102, which are demonstrably from the same large intrusion.

Each sample locality was assessed for a possible tilt correction according to rotations that may have occurred during the Laramide orogeny, when basement blocks were vertically displaced up to 7 km (Hoy and Ridgeway, 1997). However, all localities were from regions in the center of the Beartooth and Bighorn Mountain ranges, along the anticlinal axis of the basement thrust, therefore tilt corrections are negligible (less than 5°). This is apparent in the paleomagnetic pole for the Sourdough swarm, which is a high-latitude direction with remarkably high precision (Table DR2).

The Sourdough dikes also have a surprisingly large range of orientations (280 to 345°) for a swarm with such a limited extent. Some dikes in the central Bighorn Mountains have large changes in trend along their length (up to 30°). This array of orientations is shared by multiple dike swarms in the Beartooth Mountains, including both Archean and Neoproterozoic dikes. Correlation of trace element concentrations between Sourdough dikes in the two different uplifts (detailed later in supplementary text) confirms that all the Sourdough dikes are closely related geochemically, likely being from the same magmatic event as the dated dike, T09BH10.

Methods

Samples were collected in the field by drilling oriented cores or taking *in situ* oriented hand samples from mafic dikes, typically with trends of 290 to 335° and widths varying from 1 to 30 meters. One site was typically sampled in each dike, and it comprised of six to eight samples oriented with magnetic and sun compasses (when

possible). One specimen per sample was prepared and measured on an automated 2G-Enterprises DC SQuID magnetometer with $5 \times 10^{-12} \text{ A m}^2$ sensitivity per axis (Kirschvink et al., 2008), stored, and demagnetized inside a magnetically shielded room with an ambient field less than 500 nT. Measurements of the natural remanent magnetization (NRM) were followed by a series of demagnetization–measurement stages, beginning with liquid nitrogen immersion (Halgedahl and Jarrard, 1995) and followed by thermal demagnetization in 15 to 20 steps up to 580°C (or until the magnetization was randomized). Data were analyzed using free computer software packages (Cogne, 2003; Jones, 2002) and assessed using principal component analysis (Kirschvink, 1980) to calculate magnetization components and a paleomagnetic pole based upon the mean directions from each cooling unit.

The geochronologic sample (BNB09-WY-203) was collected from the same small outcrop as the paleomagnetic samples (site T09BH10). Baddeleyite was separated from a crushed sample at the University of Lund following the method of Söderlund and Johansson (2002). From the mineral separates, three aliquots of clear baddeleyite grains (3 to 6 each) were dissolved and analyzed by isotope-dilution, thermal ionization mass spectrometry (ID-TIMS) at the University of Wyoming.

Geochemical samples consisted of specimens taken from paleomagnetic cores approximately a third of a dike-width from the chilled margins. Rock samples were slabbed, crushed in a Bico Chipmunk jaw crusher, and ground to a fine powder in an agate ring mill. Whole-rock major and trace element contents were determined by fused-disc X-ray fluorescence spectrometry and solution-mode inductively coupled plasma mass spectrometry at the Ontario Geological Survey Geochemical Laboratories, Sudbury,

Ontario. The precisions of the data, based on replicate analyses of samples and blind standards, along with representative analyses, are listed in Table DR4.

Supplementary Results and Discussion

Paleomagnetism of Sourdough dikes

During demagnetization, most samples lost a considerable amount of magnetization during the liquid nitrogen immersion step, eliminating contributions from viscous remanent magnetizations (VRMs) in multi-domain magnetite (Fig. DR4). The majority of samples were single component, often with small random components being removed during low-temperature demagnetization steps (<300°C). Each site also contained mid-temperature magnetizations (300–500°C) that are identical in direction to the high-temperature components (530–576°C). Only the high-temperature components were used to calculate mean vectors because they likely represent the magnetization held by low-Ti, single-domain magnetite (Fig. DR4). One of the largest dikes, T09BH10, provides an age for the Sourdough swarm (Table DR1) along with a representative paleomagnetic direction similar to that proved primary by the baked-contact tests.

Two positive baked-contact tests confirm the high-temperature component is primary and also contain definitive thermoremanent profiles from the time of dike intrusion (Figs. DR5–7). Baked-contact tests were sampled at sites where Sourdough dikes intersected Archean(?) dikes, utilizing the predictable magnetic assemblage of mafic country rock (Fig. DR5). In both contact tests (Figs. DR6 and DR7), some samples in the “hybrid” zone yielded both baked and unbaked components. For example, in sample T11BH100-15 the baked component was held between 300 and 400°C over a dike

width away. This is predicted by half-space cooling models of dike intrusion, however the correct mineralogy (Ti-rich magnetite) is not always present to preserve a low-temperature thermoremanent magnetization (TRM) over billions of years. Considered along with robust results from 16 different cooling units, there is high confidence that the thermoremanent magnetization originates from the initial cooling of the dikes at 1899 ± 5 Ma and is sufficiently averaged to represent geographic north at the time the swarm intruded.

The only samples excluded from baked-contact tests had anomalously high NRM, likely originating from lightning strikes. These anomalously strong samples lost a majority of their magnetization during liquid nitrogen immersion, which is typical for lightning struck rocks.

Paleomagnetic poles from the Slave and Superior cratons considered for the reconstructions (Fig. 3 in main text) are shown in Table DR3. A full review of paleomagnetic poles from Slave is given in Mitchell et al. (2010). We depend mostly on the Seton and Kahochella poles because other paleomagnetic poles from Slave have large variations in declination, possibly resulting from episodes of rapid true polar wander. If this were the case (and there is not currently evidence to deny its possibility) then Wyoming and Superior would have experienced rapid changes in latitude at ca. 1.885 Ga, possibly from the pole to the equator. However, these rapid movements (or the records of them) stabilize by the time Laurentia is consolidated and have not been documented fully on other cratons.

Geochemistry of Sourdough dikes

The two major Bighorn Mountain (BH, as opposed to BT–Beartooth Mountains) dike groups (e.g., BH10 and BH61) are likely related by fractionation combined with small amounts of assimilation of upper crustal rocks (Fig. 2 in main text). The BH61-63 group is the less evolved of the two groups and has both higher Mg# and eNdT than the BH10 group (Fig. DR8). The BH10 group, more evolved, is more enriched in Th relative to La or Nb and has the lower eNdT value, consistent with an assimilated crustal component. The BH10 group also has generally higher abundances of all the incompatible elements, including elements like Ti that are not generally enriched in the upper crust, so the increase is likely due to fractionation of olivine and feldspar.

BH90 has different concentrations than the Bighorn groups - it has much more in common with the BT samples. Both BH90 and BT group have evidence of clinopyroxene fractionation, which is not evident in the other BH samples. Some incompatible elements, such as Ti, are lower in the BH60 group and BT samples than the two other BH groups, yet most highly-incompatible elements (La, Nb, Th) are higher. BH90 and the BT samples are all enriched in Th relative to Nb and La compared to the major BH groups, and along with the very negative eNdT requires a substantial crustal component in the dikes. Overall, BH90 and the BT samples are very close in composition and could represent greater crustal contributions or perhaps a second sub-swarm from different sources.

There are not enough samples to accurately distinguish the source(s) of the Sourdough dikes. It is possible that the BH10 and BH61-63 groups have an asthenospheric source magma ($eNdT > 2.0$) (Table DR5) that interacted with metasomatized lithospheric mantle before getting close to the surface. All of the samples

are low-SiO₂ basalts, around 50% SiO₂, so there is no evidence that any of the dike magmas assimilated much upper crust (high-SiO₂). BH90 and the BT dike magmas have considerably more lithospheric mantle contributions even though they are also low-SiO₂ basalts. It is possible that all of the BH and BT samples are related by mixing between asthenosphere-derived magmas and old, metasomatized lithospheric mantle (see the eNdT vs. Th/Nb plot; Fig. DR9), but more samples are needed to confirm this.

Geochronology of Wyoming craton's western and eastern margins

The Black Hills have an ambiguous relationship with Wyoming before 1.8 Ga. There are a handful of dated Archean rocks in the Black Hills, including the 2.55 Ga Little Elk granite, 2.59 Ga Bear Mountain granite (McCombs et al., 2004), and a 2.89 Ga xenocrystic zircon from the Little Elk granite (Dahl et al., 2006). In the Wyoming craton, 2.59–2.55 Ga ages are small in number but appear in five different uplifts (the Granite and Beartooth Mountains, and the Wind River, Teton, and South Madison Ranges) (Chamberlain et al., 2003; McCombs et al., 2004). This shared range of magmatic ages indicates an Archean connection between the Black Hills and Wyoming craton, possibly signifying collision with each other and the Superior craton (McCombs et al., 2004; Dahl et al., 2006). Wyoming, Superior, and the Black Hills also share similar Paleoproterozoic sedimentary sequences that suggest they could have bordered the same basin until 2.1–2.0 Ga (Roscoe and Card, 1993; Dahl et al., 2006). However, geophysical characteristics between the Bighorn Mountains and the Black Hills have been interpreted to indicate multiple Paleoproterozoic sutures and shear zones between them (Worthington et al., 2016). Our model of late Laurentian assembly, proposes that the ultimate juxtaposition

(and present-day positions) of the Wyoming and the Black Hills occurred during the final suturing between the Wyoming and Superior cratons, ca. 1.715 Ga (Nabelek et al., 2001). This likely resulted in changes in stress directions recorded by rocks in the Cheyenne belt (SE Wyoming) that show dramatic changes in transpressional deformation at 1.78 and 1.75 Ga, interrupted briefly by syn-collisional extension (Sullivan and Beane, 2013). The Black Hills may have remained proximal to Superior or Wyoming after rifting (>2.0 Ga) only to be caught between the two block during their final collision ca. 1.715 Ga.

The eastern boundary of the Wyoming craton, as defined in Figure 1 of the main text, is based primarily upon the geophysical interpretations of Worthington et al. (2016) in the vicinity of the Bighorn Mountain. We have extrapolated this Archean-Proterozoic boundary to the NNW with a slight bend to the north so that the border intersects the eastern edge of the MHB, which is defined by subsurface anomalies (Boerner et al., 1998). The northern extension of this boundary cuts through central Montana, roughly following linear discontinuities in aeromagnetic maps, but will require further research to accurately define.

The southern extension of Wyoming's eastern margin ends at the Cheyenne belt, which marks the suture with the Yavapai block. In our model, the Cheyenne belt does not extend into South Dakota; this would require an extension of the Wyoming craton into South Dakota, also. Most older models that connect 1.77-1.76 Ga deformation in the Black Hills and Hartville Uplift with the Cheyenne belt do not incorporate geophysical trends in the subsurface as well as our model and others (Worthington et al., 2016).

It is unknown how far the Archean (Wyoming) craton's western margin extends. Archean rocks crop out in south-central Idaho (Albion Range) and eastern Nevada (East

Humboldt Range) and are assumed to underlie parts of the Snake River Plain, but are separated from Wyoming by the deformed Paleoproterozoic Farmington zone (Bryant, 1988; Mueller et al., 2011; Nelson et al., 2002). These westernmost Archean rocks may be a separate terrane (the Grouse Creek Block) that possibly shared an earlier (>2.45 Ga) history with Wyoming or subsequently joined during the assembly of Laurentia (Foster et al., 2006; Mueller et al., 2004).

SUPPLEMENTARY FIGURES

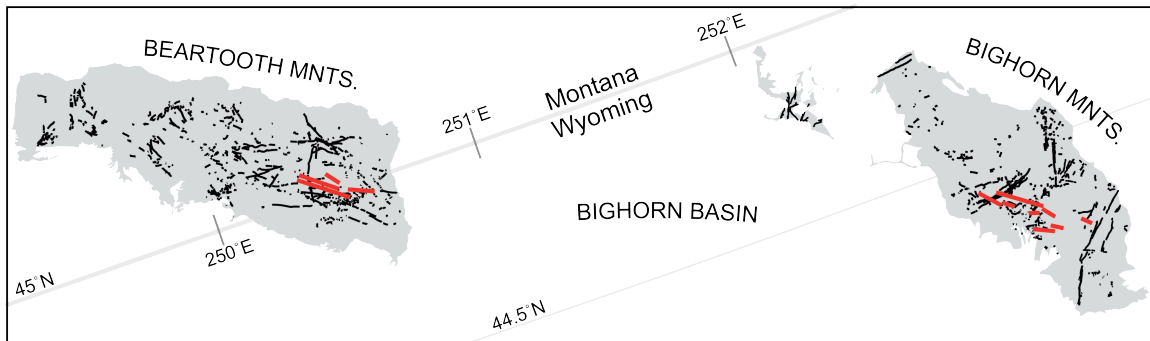


Figure DR1. Map of identified Sourdough dikes (red) spanning two Precambrian uplifts, slightly exaggerated in size for better visibility. Other undifferentiated dikes are colored in black. The Sourdough dikes appear to be nearly in line with each other across the Bighorn basin, suggesting that neither uplift was rotated during exhumation. Maps modified from Prinz (1964), Lopez (2001), Berg et al. (1999), Osterwald (1978), Ross and Heimlich (1972), Armbrustmacher (1977), Hinrichs et al. (1990), Heimlich et al. (1973), and Barker (1982).

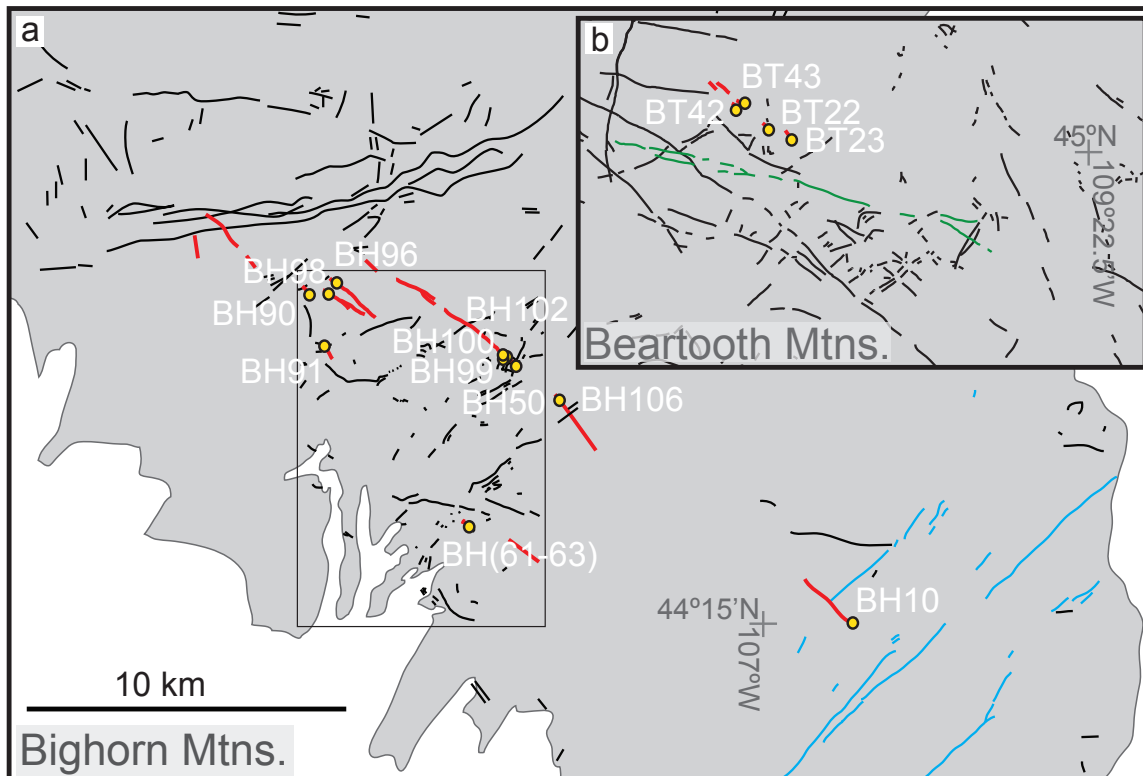


Figure DR2. Detailed maps of sampling localities (yellow dots) for Sourdough dikes (red) in the Beartooth and Bighorn Mountains. Both maps have the same length scale, with gray representing Precambrian rock and white representing Phanerozoic rocks. Site IDs are labeled in white. Thin gray rectangle defines extent of the Lake Helen quadrangle in Figure DR3. Powder River dikes (ca. 2152 to 2161 Ma) are colored in blue, Gunbarrel dikes (ca. 780 Ma) are colored in green, and undifferentiated dikes are colored black, many of which are likely Archean. Sites BH61, BH62, and BH63 are three small dikes (<1.5 m wide) within 100 m of each other. Maps modified from Armbrustmacher (1977); Barker (1982); Hinrichs et al. (1990); Lopez (2001); Prinz (1964).

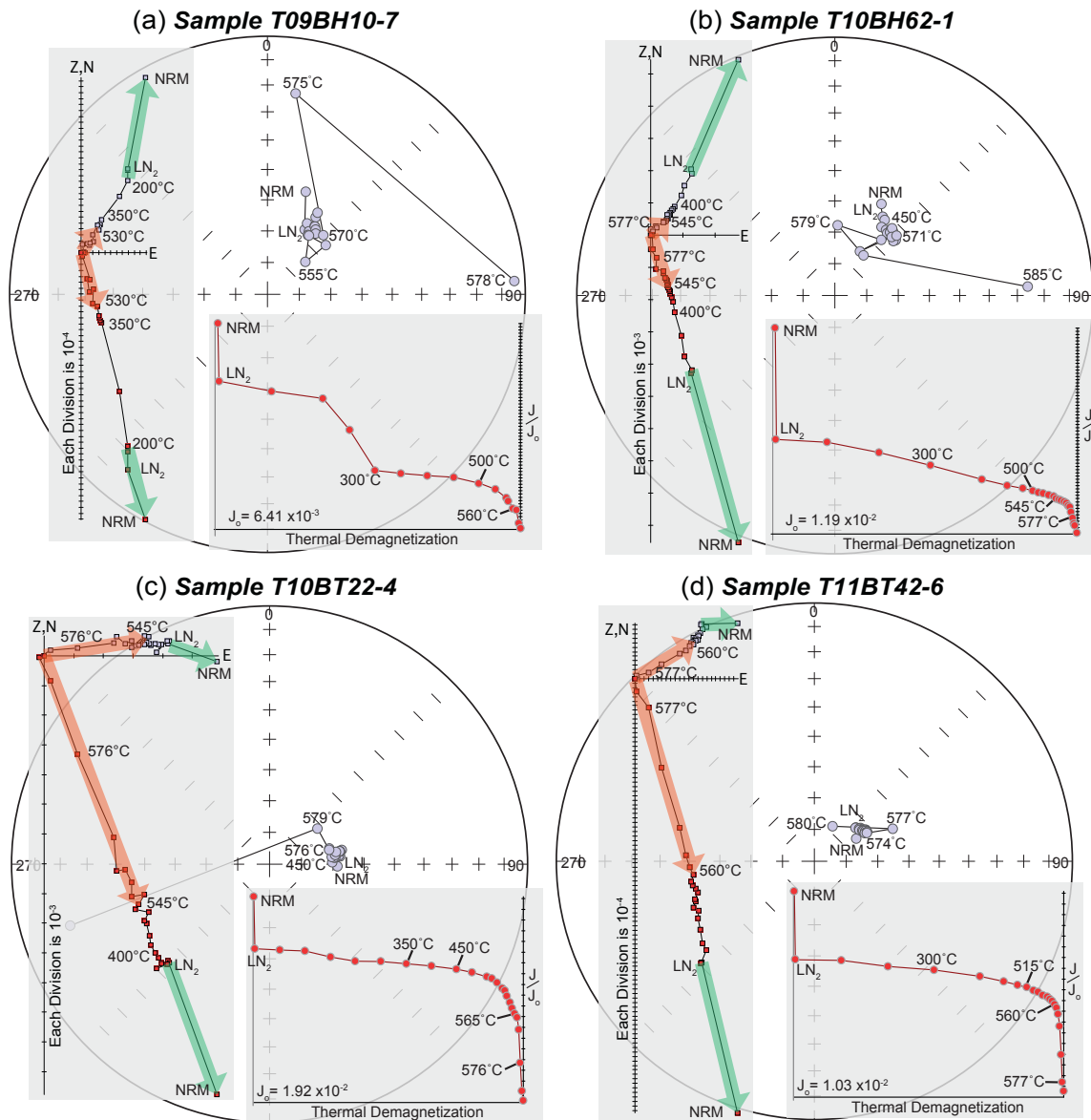


Figure DR4. Representative demagnetization data for the Sourdough swarm from two different sites in each uplift. For each sample (a-d) an equal-area plot, an orthographic plot, and a moment vs. thermal demagnetization step plot are shown. Vectors are fit to magnetization components observed through different unblocking temperatures. Orange vectors indicate the primary magnetization and green vectors represent the random VRMs of no significant importance. Primary component vectors are fit to data that likely represent the unblocking of Ti-poor magnetite. Blue circles on the equal-area plots indicate positive inclinations and red symbols indicate negative inclinations. On the orthogonal plots, red squares indicate inclination direction and blue squares represent declination.

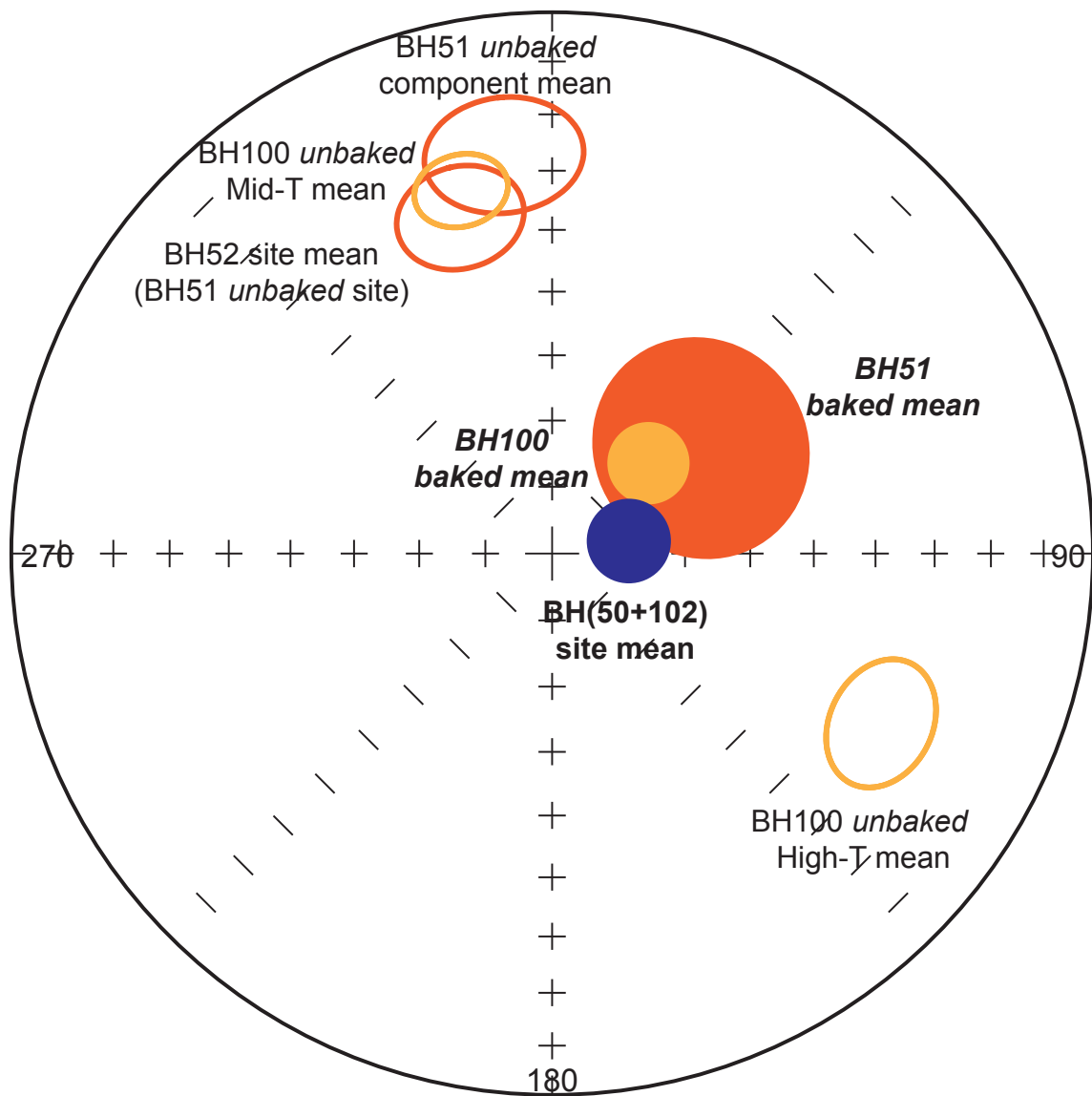


Figure DR5: Site mean results from two baked-contact tests for the same dike, BH50/BH102, into different older mafic dikes. In the case of BH100, two unbaked components were present in the host rock, which is similar to other Archean(?) dikes in the area. Samples nearest to the baked contact contain a strong baked component very similar to the mean direction for the Sourdough dike (BH50/BH102).

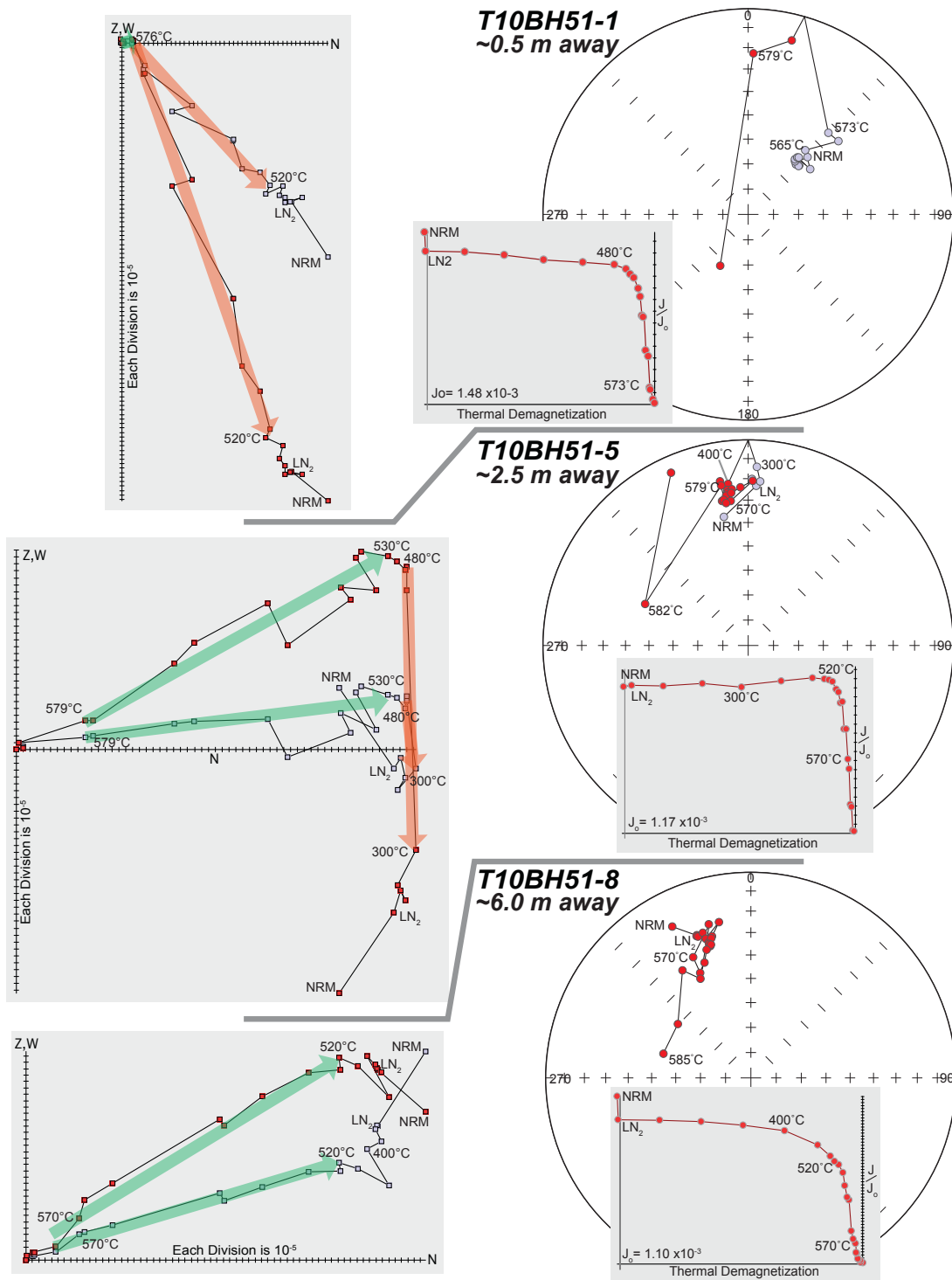


Figure DR6. Demagnetization data of the baked-contact test BH51 for Sourdough dike BH50 (also BH102). The test was sampled into an Archean(?) dike with a fully unbaked site named BH52. Approximate distance from baked contact is shown along next to sample label (intruding dike is ~7 m wide). The baked component vectors are shown in orange and the host rock unbaked magnetization is shown in green. A small unbaked component still remains in samples ~0.5 m from the intruding dike, suggesting temperatures never completely surpassed the unblocking temperature for magnetite.

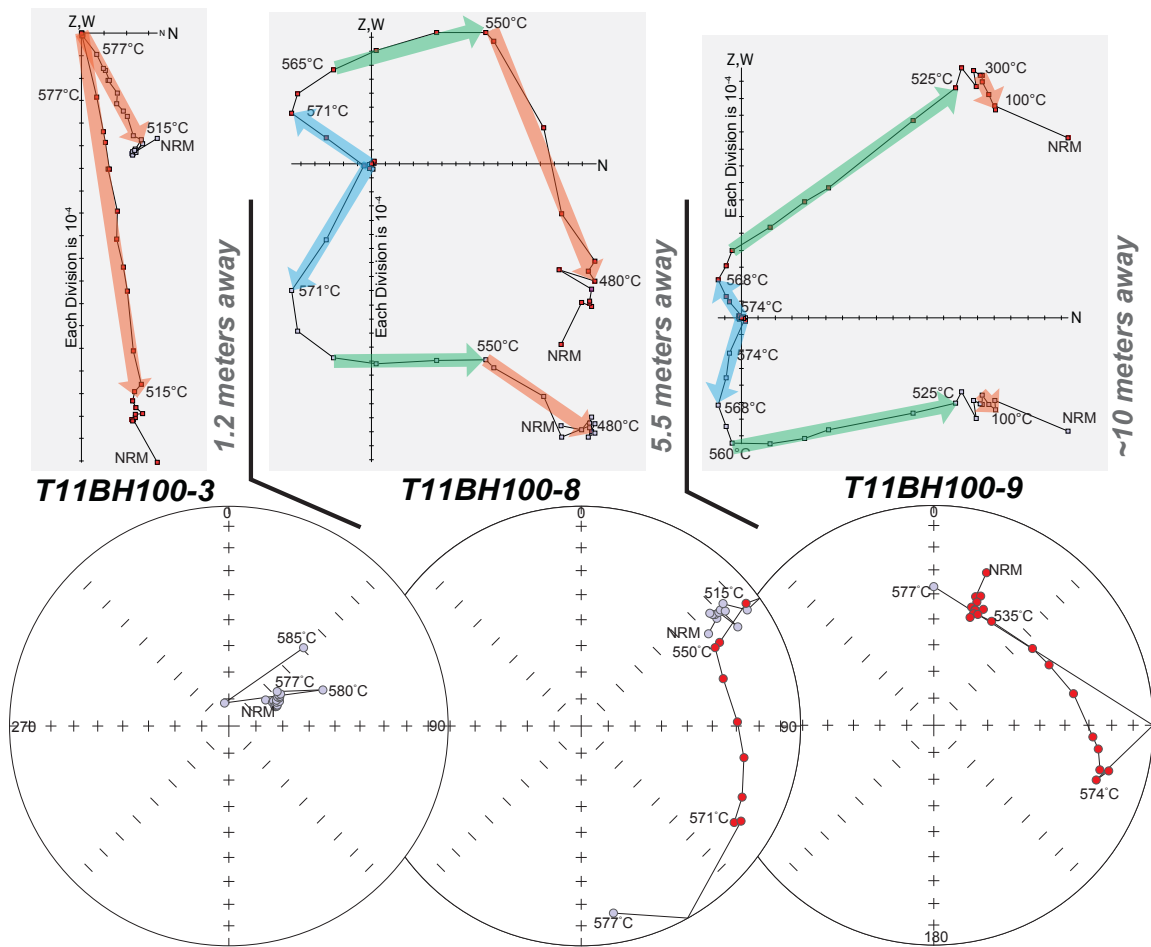


Figure DR7. Demagnetization data from baked-contact test BH100 for Sourdough dike BH102 (also BH50). The test was sampled into an older Archean(?) dike that is cross-cut by dike BH102/BH50. There are two unbaked components present in the Archean dike (blue and green vectors), both of which are completely overprinted by the baked component (orange vectors) less than 1.2 m from the baked-contact. Distance from baked-contact is given for each sample, with important demagnetization steps labeled with corresponding temperatures. A small baked component can be seen at low temperatures over a dike width away from the baked contact. This indicates that a large assemblage of stable magnetic carriers is present in the Archean dike, none of which has experienced a significant amount of heating since the intrusion of the Sourdough swarm.

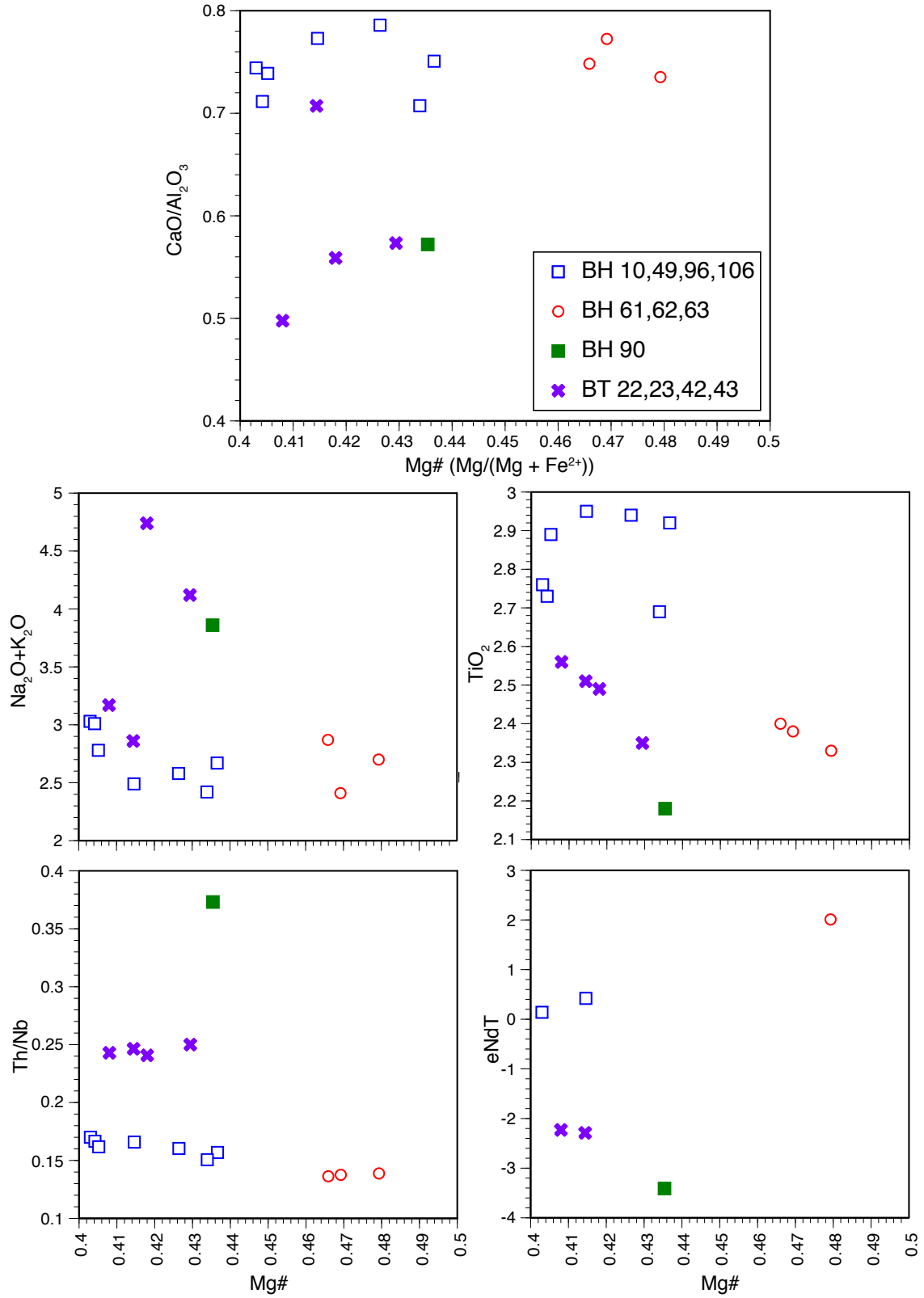


Figure DR8. Geochemical variation within samples from the Sourdough dike swarm comparing concentrations for groups of dikes with slightly different affinities.

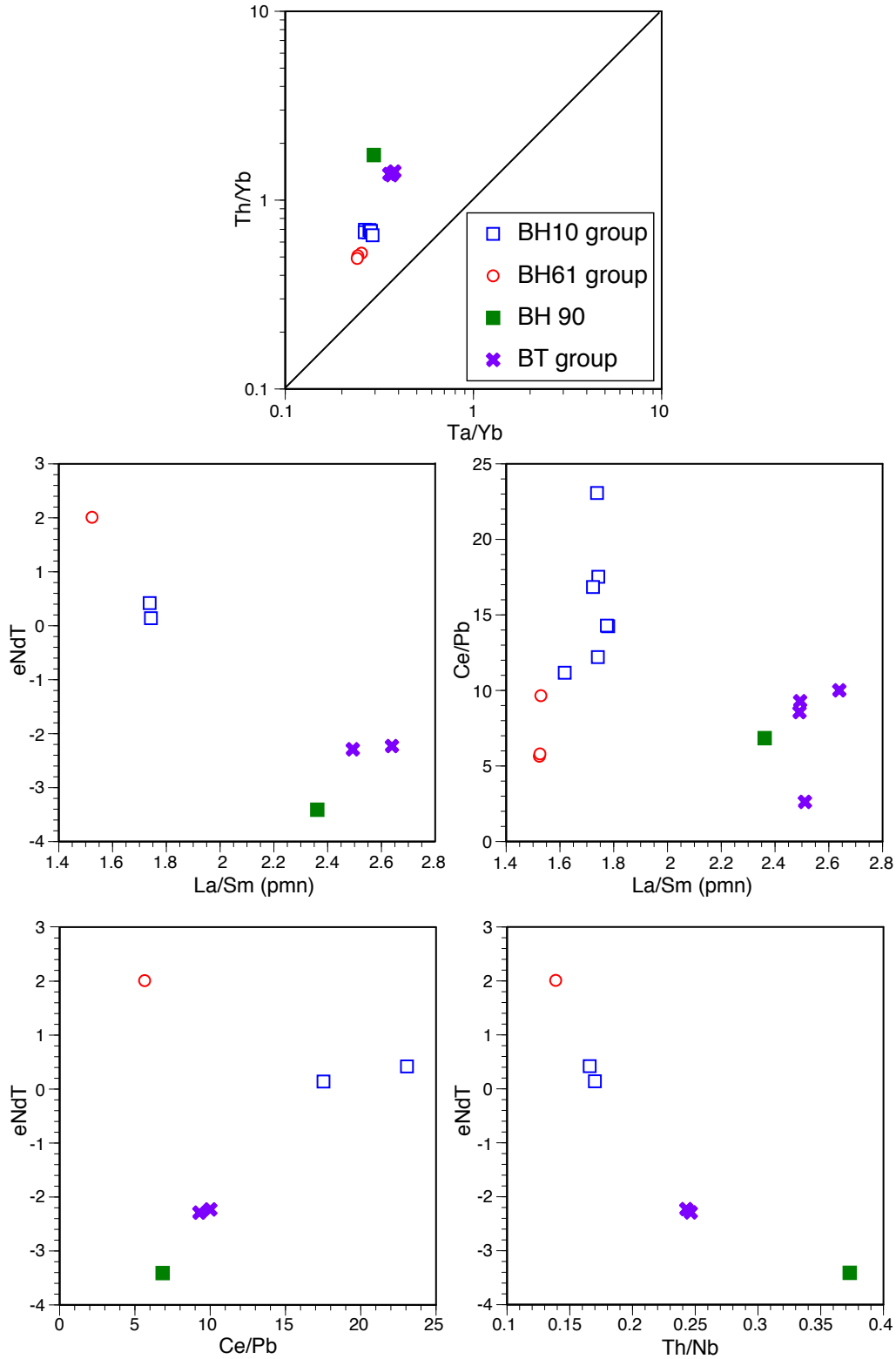


Figure DR9. Geochemical variation within samples from the Sourdough dike swarm comparing concentrations of Th/Yb, Ta/Yb, La/Sm, Ce/Pb, Ce/Pb, Th/Nb and $^{143}\text{Nd}/^{144}\text{Nd}$ ratios relative to the depleted mantle reservoir model (eNdT). Colors correspond to Fig. DR8.

TABLE DR2. PALEOMAGNETIC DATA FOR THE SOURDOUGH DIKE SWARM

ID	Width (m)	Trend (°)	Site Lat.(N)		Site Long.(W)		Dec. (°)	Inc. (°)	a95 (°)	n(p)/N	k	Plat. (°N)	Plong. (°E)	A95 (°)	Tunb (°C)
			deg.	min.	deg.	min.									
T09BH10	~30	335	44	14.982	106	57.465	57.1	76.9	9.6	7(1)/8	37.2	52.8	288.9	17.2	500-555
T10BT22	1	295	45	0.557	109	32.312	101.3	73.8	5.2	5/6	173.8	32.8	286.3	8.9	450-575
T10BT23	10	315	45	0.405	109	31.718	21.3	82.3	10.9	3/6	83.8	58.7	261.0	21.0	500-580
T11BT42	0.14	290	45	0.940	109	33.108	37.9	74.8	4.5	8/8	134.0	62.6	290.0	7.8	550-574
T11BT43	0.7	300	45	0.961	109	33.121	77.8	78.6	5.4	6/8	157.0	45.4	281.8	9.9	560-577
T10BH49	~5	345	44	20.423	107	8.392	109.7	78.0	8.6	7/8	43.4	33.3	279.0	15.6	545-568
<i>T10BH50</i>	7	320	44	20.711	107	8.411	81.2	77.2	7.7	8/8	46.7	43.0	286.8	13.8	540-575
T10BH61	0.5	290	44	17.164	107	9.930	257.6	-67.3	13.2	3/8	58.6	-39.4	127.0	20.1	530-582
T10BH62	0.5	295	44	17.150	107	9.945	25.1	70.0	7.1	8/8	53.9	71.1	303.2	11.4	520-580
T10BH63	2.5	285	44	17.150	107	9.945	87.8	69.8	7.3	5/8	88.9	35.4	299.4	11.6	520-570
T11BH90	1.3	330	44	22.263	107	14.816	32.5	64.9	3.4	8/8	232.2	67.3	324.9	4.9	450-573
T11BH91	6	345	44	20.951	107	14.173	35.5	59.9	4.8	7/8	134.3	63.8	338.1	6.4	550-580
T11BH96	1.4	315	44	22.506	107	14.041	97.9	69.5	4.0	8/8	171.4	30.1	296.0	6.3	480-571
T11BH98	~10	330	44	22.208	107	14.204	56.8	73.0	5.9	6/6	109.5	53.2	299.5	9.9	565-576
T11BH99	0.3	320	44	20.794	107	8.560	61.5	79.7	3.9	7/8	201.6	50.7	281.1	7.4	500-576
<i>T11BH102</i>	7.5	320	44	20.800	107	8.551	79.7	79.8	12.6	6(1)/8	26.3	44.5	280.7	23.5	540-580
T11BH106	~20	315	44	20.033	107	6.987	108.8	74.6	6.4	7/8	77.7	30.1	284.7	11.1	450-515
BH50+BH102	7-7.5	320	N.A.*	N.A.*	N.A.*	N.A.*	80.2	78.3	6.5	14(1)/16	39.3	43.8	284.4	11.5	540-580
<i>Mean (All)</i>							65.1	75.2	4.7	16	21.8	49.2	292.0	8.1	
<i>Bighorn Mean (ex. BH90)</i>							69.7	74.3	5.8	11	22.7	46.6	294.2	9.8	
<u>Sites used for baked-contact tests</u>															
T10BH51 (bkd)	2.5	35	44	20.711	107	8.411	54.7	62.1	16.5	5/9	18.0	51.3	324.3	22.6	200-480 and 400-573
T10BH51 (unbkd)	2.5	35	44	20.711	107	8.411	353.1	-26.5	10.2	4(1)/9	67.6	-31.4	260.6	8.1	520-578
T11BH100 (bkd)	3	65	44	20.801	107	8.568	46.8	70.1	6.2	7/15	97.3	58.6	307.9	9.8	N.D [†]
T11BH100 (unbkdMT)	3	65	44	20.801	107	8.568	345.9	-31.4	6.2	9/15	70.2	-27.4	268.0	5.2	515-565
T11BH100 (unbkdHT)	3	65	44	20.801	107	8.568	117.3	-31.9	8.8	7/15	48.1	31.4	156.6	7.4	568-580
T11BH100 (unbkdLT)	3	65	44	20.801	107	8.568	64.2	68.3	10.4	4/15	79.2	47.8	309.3	16.1	200-480
<i>Note: Italicized sites represent dikes yielding positive baked-contact tests, both sampled at intersections with older mafic dikes. Coordinates in WGS84.</i>															
<i>Dec.(Inc.) = declination (inclination) of mean magnetization, a95 (A95) = 95% confidence interval of mean direction in local (pole) coordinates. n=# of samples</i>															
<i>(p=plane-fits) used in mean, N=# of samples collected, k=precision parameter, Plat. (Plong.) = paleolatitude (paleolongitude) of paleomagnetic pole,</i>															
<i>Tunb=unblocking temperature range of magnetization, bkd="baked" magnetization, unbkd="unbaked magnetization.</i>															
<i>*N.A. = not applicable, this site is the average of the two localities indicated that are from different portions of a dike along its length</i>															
<i>†N.D.= multiple discrete temperature ranges represent this baked-contact test's unblocking spectrum, so no single range is defined</i>															

TABLE DR3. PALEOMAGNETIC POLES USED/CONSIDERED IN RECONSTRUCTION

Rock/Formation	ID	Plat (°N)	Plong (°E)	A95 (°)	Age (Ma)	References
<u>Slave</u>						
Martin Fm lavas (Rae [†])	Marti	-9	288	8.5	1818±4	Evans and Bingham (1973)
Sparrow dikes (Rae [†])	Spar	12	291	7.9	1827±4	McGlynn <i>et al.</i> (1974), Bostok and van Breeman (1992)
Et-Then Grp	Et	4	310	8	ca. 1780(?)	Irving <i>et al.</i> (1972)*
Tochatwi Fm	Toch	-14	204	12	ca. 1885-1870	Evans and Bingham (1976)*
Stark Fm	Star	-11	199	8	ca. 1885-1870	Evans <i>et al.</i> (1980)*
Douglas Peninsular Fm	DougP	-17	245	16	ca. 1885-1870	Irving and McGlynn (1979)*
Pearson Fm basalts	Pearson	-22	269	6	1870±4	McGlynn and Irving (1978)*
Kahochella Grp	Kahoch	-12	285	7	1882±4	Reid <i>et al.</i> (1981)*
Ghost dikes	Ghost	2	254	6	1886±5	Buchan <i>et al.</i> (2016)
Seton Fm volcanics	Seton	-6	260	4	1885±5	Irving and McGlynn (1979)*
Rifle Fm	Rifle	19	353	9	1963±6	Evans and Hoyer (1981)*
Indin dikes	Indin	36	284	7	2126-2108	Buchan <i>et al.</i> (2016)
<u>Superior</u>						
Cleaver dikes	Cleav	19.4	276.7	6.1	1736-1745	Irving <i>et al.</i> (2004)
Post-Hudsonian mean	P-Hud	21	265	5.2	ca. 1750	Irving <i>et al.</i> (2004)
Dubawnt Grp	Dubaw	7	277	8	1800-1830	Park <i>et al.</i> (1973), Rainbird and Davis (2007)
Laurentian Mean 1870 Ma	LM1870	1	245.8	3.9	1870±1	Schmidt (1980), Hamilton <i>et al.</i> (2009)
Molson dikes	Mols	36.6	209.8	3.8	1877+7/-4	Zhai <i>et al.</i> (1994), Halls and Heaman (2000), Evans and Halls (2010)
Minto dikes	Mint	38.7	171.5	13.1	1998±2	Buchan <i>et al.</i> (1998), Evans and Halls (2010)
Marathon dikes, Normal	Marath-N	54.1	188.9	7.7	2126-2121	Buchan <i>et al.</i> (1996), Halls <i>et al.</i> (2008), Evans and Halls (2010)
Biscotasing dikes	Bisco	26	223.9	7	2172-2167	Buchan <i>et al.</i> (1993), Halls and Davis (2004), Evans and Halls (2010)
<u>Wyoming</u>						
Rabbit Creek-Powder River-South Pass dikes	RC-PR	65.5	339.2	7.6	2171-2152	Kilian <i>et al.</i> (2015)
Sourdough dikes	SD	49.2	291	8.1	ca. 1900	<i>this study</i>
<i>Note: All paleopoles older than 1875 Ma from Superior are given in the Eastern Superior reference frame, see Evans and Halls (2010).</i>						
<i>*Reviewed, corrected, and recalculated by Mitchell <i>et al.</i> (2010).</i>						
<i>†Units are located in the Rae craton, but are used for the Slave craton reference frame because the cratons unite at ca. 1.9 Ga.</i>						

TABLE DR4. GEOCHEMICAL RESULTS FROM THE BIGHORN AND BEARTOOTH MOUNTAINS DIKES

d,w	BH10 8,30+	BH49 7,5+	BH50 2,7	BH61 0,2,0,5	BH62 0,2,0,5	BH63 0,7,2,5	BH90 0,4,1,3	BH96 0,4,1,4	BH98 1,4,5-10	BH99 0,1,0,3	BH106 7,20-25	BT22 0,3,1	BT23 3,10	BT42 0,04,0,14	BT43 0,2,0,7	Int. Std.	1σ
SiO ₂	48.96	49.18	48.33	49.70	49.81	49.56	49.40	49.14	48.72	48.65	49.85	47.36	47.74	48.35	47.36	50.5	0.36
TiO ₂	2.71	2.69	2.88	2.28	2.36	2.32	2.12	2.85	2.86	2.63	2.87	2.41	2.42	2.44	2.26	2.45	0.03
Al ₂ O ₃	12.31	12.42	12.14	12.68	12.71	12.56	13.92	12.07	12.01	12.25	11.93	12.91	13.09	12.97	13.26	13.64	0.09
Fe ₂ O ₃ ^T	16.62	16.80	16.56	14.58	14.83	14.76	14.58	17.15	16.38	16.91	15.39	15.98	16.08	16.47	15.96	13.41	0.05
MnO	0.22	0.22	0.20	0.18	0.17	0.19	0.20	0.22	0.21	0.18	0.19	0.22	0.22	0.20	0.22	0.24	0
MgO	5.10	5.18	5.33	6.10	5.88	5.93	5.11	5.31	5.77	5.89	5.20	5.14	5.25	5.16	5.46	4.02	0.05
CaO	9.16	8.84	9.38	9.32	9.51	9.70	7.96	8.92	9.02	8.67	9.38	9.13	7.32	6.46	7.60	7.47	0.11
Na ₂ O	2.19	2.07	1.79	1.84	2.21	2.00	2.34	1.95	2.11	1.83	2.11	1.83	3.30	1.85	2.47	3.16	0.05
K ₂ O	0.79	0.90	0.64	0.80	0.61	0.35	1.42	0.79	0.50	0.54	0.41	0.92	1.30	1.17	1.50	1.85	0.04
P ₂ O ₅	0.29	0.30	0.32	0.24	0.25	0.24	0.25	0.32	0.33	0.29	0.31	0.30	0.29	0.30	0.27	1.17	0.01
LOI	1.11	0.91	1.82	1.53	1.39	1.64	1.87	0.80	1.52	1.90	1.66	3.10	2.25	3.40	2.54	1.62	0.33
Total	99.46	99.51	99.39	99.25	99.73	99.25	99.18	99.53	99.42	99.74	99.30	99.30	99.25	98.76	98.90	99.53	---
Mg#	0.403	0.404	0.415	0.479	0.466	0.469	0.435	0.405	0.437	0.434	0.426	0.414	0.418	0.408	0.429	0.397	0
V	386	359	370	378	378	388	288	378	383	365	376	357	369	364	351	337	13
Cr	173	108	110	143	130	121	99	86	91	95	86	117	100	102	109	19	5
Co	51.5	51.5	48.5	45.3	43.9	45.3	50.8	51.5	54	53.8	42.8	51	49.8	47.4	53	29	3
Ni	71	69	67	89	87	86	54	68	66	73	62	44	44	43	51	12	3
Zn	126.4	151.0	130.4	140.8	121.2	107.2	100.3	150.4	139.6	128.7	131.5	121.4	130.1	134.4	140.4	133	7
Rb	23.2	21.2	18.7	30.0	20.8	12.6	54.5	28.5	14.2	16.9	12.7	20.5	49.3	47.1	61.5	40	3
Sr	199	223	215	183	208	207	186	177	171	204	196	207	185	154	200	408	5
Y	40.0	40.1	42.1	34.3	35.3	35.4	27.6	42.1	44.2	37.9	41.7	31.9	31.9	32.2	29.8	47	4
Zr	229	225	238	167	174	160	143	236	241	186	241	169	160	148	146	149	5
Nb	15.5	15.4	16.5	11.9	12.3	11.9	12.6	16.4	16.9	14.9	16.7	16.5	17.0	16.9	15.4	8	1
Ba	182.2	227.8	177.5	439.6	191.5	97.4	383.1	209.1	110.8	195.3	155.6	496	763.1	1312.7	1141.8	2202	143
La	21.22	21.14	22.4	14.71	15.32	15	20.79	22.17	22.88	20.62	20.55	25.54	25.13	27.44	24.05	26.68	0.55
Ce	50.82	50.54	53.06	36.13	37.69	36.68	43.1	52.49	54.15	48.59	50.27	53.85	53.1	57.04	50.37	58.55	0.21
Pr	7.02	7.08	7.49	5.22	5.5	5.28	5.7	7.34	7.53	6.78	7.14	6.93	6.73	7.32	6.52	8.41	0.08
Nd	31.55	31.63	33.33	24.06	24.98	24.46	24.14	32.95	33.49	30.58	32.08	28.57	28.68	30.69	27.12	39.39	0.42
Sm	7.87	7.93	8.33	6.24	6.49	6.34	5.69	8.23	8.31	7.51	8.21	6.62	6.52	6.72	6.19	9.47	0.06
Eu	2.4	2.37	2.53	2.07	2.24	2.03	1.8	2.42	2.49	2.24	2.4	2.11	2.1	2.11	1.99	3.82	0.1
Gd	8.38	8.35	8.82	6.98	7.21	7.09	5.68	8.74	8.87	8.01	8.59	6.58	6.4	6.9	6.26	9.92	0.35
Tb	1.287	1.306	1.375	1.09	1.124	1.106	0.859	1.363	1.385	1.235	1.348	0.99	0.984	1.026	0.953	1.45	0.02
Dy	7.95	8.14	8.45	6.8	6.98	6.96	5.4	8.36	8.49	7.55	8.19	6.16	6.09	6.35	5.79	8.81	0.16
Ho	1.56	1.55	1.62	1.3	1.36	1.36	1.04	1.6	1.63	1.45	1.59	1.2	1.18	1.22	1.12	1.76	0.01
Er	4.38	4.36	4.64	3.65	3.8	3.78	2.97	4.53	4.54	4	4.56	3.43	3.34	3.45	3.23	4.94	0.01
Tm	0.591	0.597	0.628	0.506	0.518	0.53	0.418	0.613	0.627	0.544	0.624	0.471	0.463	0.471	0.442	0.68	0.01
Yb	3.77	3.78	3.93	3.15	3.29	3.32	2.71	3.86	3.86	3.44	3.96	3.00	2.90	2.95	2.80	4.33	0.06
Lu	0.54	0.55	0.57	0.45	0.47	0.48	0.4	0.56	0.57	0.5	0.58	0.45	0.43	0.41	0.39	0.64	0.02
Cs	0.86	0.53	0.84	0.46	0.4	0.6	0.51	1.04	0.52	0.54	0.5	0.58	1.09	0.89	1.78	1.73	0.04
Hf	6.01	5.88	6.29	4.46	4.65	4.44	3.86	6.12	6.15	5.15	6.19	4.51	4.22	4.08	3.98	4.09	0.05
Ta	1	1	1.1	0.8	0.8	0.8	0.8	1.1	1.1	1	1.1	1.1	1.1	1.1	1	0.47	0.03
Th	2.63	2.56	2.73	1.65	1.67	1.63	4.69	2.65	2.65	2.24	2.67	4.07	4.1	4.1	3.85	4.08	0.32
U	0.72	0.71	0.8	0.46	0.51	0.46	1.1	0.73	0.73	0.59	0.76	0.75	0.77	0.82	0.71	1.52	0.11
Sc	34.7	34.5	34.9	35.8	34.7	36.3	32.5	35	36	34.6	36.2	37.2	36.6	37	36	37.6	0.5
Pb	2.9	3	2.3	6.4	6.5	3.8	6.3	4.3	3.8	3.4	4.5	5.8	6.2	5.7	19.2	6.95	0.07

Note: Major oxides by XRF in wt. %, trace elements by ICP-MS in weight ppm, and LOI = loss on ignition. Mg# = Mg/(Mg+Fe²⁺). Int. Std. is standard basalt from Lake Tahoe, California submitted as blind standard. Precision is shown in final column, 1σ (S.D.). d = estimated distance (in meters) of sample from the closest margin of the dike, w = total width of dike (in meters). ? = unknown distance from margin of dike, given when measurement uncertainty precludes a meaningful estimate.

TABLE DR5. ISOTOPIC DATA FOR SELECTED SOURDOUGH DIKES

	Sm (ppm)	Nd (ppm)	$^{147}\text{Sm}/^{144}\text{Nd}$	$^{143}\text{Nd}/^{144}\text{Nd}_m$	2-sigma	$\epsilon_{\text{Nd}} \text{ pres}$	$^{143}\text{Nd}/^{144}\text{Nd}(T)$	$\epsilon_{\text{Nd}}(T)$	Tdm (Ma)
BH10	7.72	30.73	0.1518	0.512084	0.000008	-10.81	0.510187	0.14	2521
BH50	7.90	31.57	0.1513	0.512092	0.000008	-10.64	0.510200	0.42	2483
BH61	5.90	22.75	0.1568	0.512242	0.00001	-7.73	0.510281	2.01	2325
BH90	5.36	23.16	0.1400	0.511755	0.000008	-17.22	0.510005	-3.41	2793
BT22	6.17	27.39	0.1362	0.511765	0.000014	-17.03	0.510061	-2.29	2640
BT42	6.46	28.93	0.1351	0.511754	0.000007	-17.25	0.510065	-2.23	2624

Note: m=measured; pres=present day; T=ratio at time of crystallization at 1900 Ma, based on the U-Pb age (this study); Tdm=depleted mantle model age.

SUPPLEMENTARY REFERENCES

- Armbrustmacher, T. J., 1977, Geochemistry of Precambrian mafic dikes, central Bighorn Mountains, Wyoming, U.S.A: *Precambrian Research*, v. 4, no. 1, p. 13-38.
- Barker, F., 1982, Geologic map of the Lake Helen quadrangle, Big Horn and Johnson Counties, Wyoming: USGS Geologic Quadrangle Map 1563.
- Berg, R. B., Lonn, J. D., and Locke, W. W., 1999, Geologic map of the Gardiner 30' x 60' quadrangle, south-central Montana: Montana Bureau of Mines and Geology Open File Report 387.
- Bleeker, W., Hamilton, M., and Söderlund, U., 2008, Towards a complete magmatic event "barcode" for the Slave craton, II: The ca. 1884 Ma Ghost swarm: *Geological Association of Canada-Mineralogical Association of Canada Abstracts*, v. 33.
- Boerner, D.E., Craven, J.A., Kurtz, R.D., Ross, G.M., and Jones, F.W., 1998, The Great Falls Tectonic Zone: suture or intracontinental shear zone?: *Canadian Journal of Earth Sciences*, v. 35, no. 2, p. 175-183.
- Bostock, H., and Van Breemen, O., 1992, The timing of emplacement, and distribution of the Sparrow diabase dyke swarm, District of Mackenzie, Northwest Territories: *Geological Survey of Canada Paper 92-2*, v. Report 6, p. 49-56.
- Bryant, B., 1988, Geology of the Farmington Canyon complex, Wasatch Mountains, Utah: U.S. Geological Survey Professional Paper 1476, p. 54.
- Buchan, K.L., Mitchell, R.N., Bleeker, W., Hamilton, M.A., and LeCheminant, A.N., 2016, Paleomagnetism of ca. 2.13–2.11 Ga Indin and ca. 1.885 Ga Ghost dyke swarms of the Slave craton: Implications for the Slave craton APW path and

relative drift of Slave, Superior and Siberian cratons in the Paleoproterozoic: *Precambrian Research*, v. 275, p. 151-175.

Buchan, K. L., Mortensen, J. K., Card, K. D., and Percival, J. A., 1998, Paleomagnetism and U–Pb geochronology of diabase dyke swarms of Minto block, Superior Province, Quebec, Canada: *Canadian Journal of Earth Sciences*, v. 35, p. 1054-1069.

Buchan, K.L., Halls, H.C., and Mortensen, J.K., 1996, Paleomagnetism, U–Pb geochronology, and geochemistry of Marathon dykes, Superior Province, and comparison with the Fort Frances swarm: *Canadian Journal of Earth Sciences*, v. 33, no. 12, p. 1583-1595.

Buchan, K.L., Mortensen, J.K., and Card, K.D., 1993, Northeast-trending Early Proterozoic dykes of southern Superior Province: multiple episodes of emplacement recognized from integrated paleomagnetism and U–Pb geochronology: *Canadian Journal of Earth Sciences*, v. 30, no. 6, p. 1286-1296.

Chamberlain, K. R., Frost, C. D., and Frost, B. R., 2003, Early Archean to Mesoproterozoic evolution of the Wyoming Province: Archean origins to modern lithospheric architecture: *Canadian Journal of Earth Sciences*, v. 40, p. 1357-1374.

Cogne, J. P., 2003, PaleoMac: A Macintosh™ application for treating paleomagnetic data and making plate reconstructions.: *Geochemistry, Geophysics, Geosystems*, v. 4, no. 1.

Corrigan, D., Pehrsson, S., Wodicka, N., and de Kemp, E., 2009, The Palaeoproterozoic Trans-Hudson Orogen: a prototype of modern accretionary processes: *Geological Society, London, Special Publications*, v. 327, no. 1, p. 457-479.

- Dahl, P.S., Hamilton, M.A., Wooden, J.L., Foland, K.A., Frei, R., McCombs, J.A., and Holm, D.K., 2006, 2480 Ma mafic magmatism in the northern Black Hills, South Dakota: A new link connecting the Wyoming and Superior cratons: *Canadian Journal of Earth Sciences*, v. 43, p. 1579-1600.
- Evans, D. A. D., and Halls, H. C., 2010, Restoring Proterozoic deformation within the Superior craton: *Precambrian Research*, v. 183, no. 3, p. 474-489.
- Evans, M. E., and Bingham, D. K., 1973, Paleomagnetism of the Precambrian Martin Formation, Saskatchewan: *Canadian Journal of Earth Sciences*, v. 10, no. 10, p. 1485-1493.
- , 1976, Paleomagnetism of the Great Slave Supergroup, Northwest Territories, Canada: the Tochatwi Formation: *Canadian Journal of Earth Sciences*, v. 13, no. 4, p. 555-562.
- Evans, M. E., and Hoye, G. S., 1981, Paleomagnetic results from the lower Proterozoic rocks of Great Slave Lake and Bathurst inlet areas, Northwest Territories., *in* Campbell, F. H. A., ed., *Proterozoic Basins of Canada*, Geological Survey of Canada Papers, p. 191-202.
- Evans, M. E., Hoye, G. S., and Bingham, D. K., 1980, The paleomagnetism of the Great Slave Supergroup: the Akaitcho River Formation: *Canadian Journal of Earth Sciences*, v. 17, no. 10, p. 1389-1395.
- Foster, D. A., Mueller, P. A., Mogk, D. W., Wooden, J. L., and Vogl, J. J., 2006, Proterozoic evolution of the western margin of the Wyoming craton: implications for the tectonic and magmatic evolution of the northern Rocky Mountains: *Canadian Journal of Earth Sciences*, v. 43, no. 10, p. 1601-1619.

- Gordon, T., Hunt, P., Bailes, A., and Syme, E., 1990, U–Pb ages from the Flin Flon and Kiseeynew belts, Manitoba: chronology of crust formation at an Early Proterozoic accretionary margin: The Early Proterozoic Trans-Hudson Orogen of North America. Edited by JF Lewry and MR Stauffer. Geological Association of Canada, Special Paper, v. 37, p. 177-199.
- Halgedahl, S. L., and Jarrard, R. D., 1995, Low-temperature behavior of single-domain through multidomain magnetite: Earth and Planetary Science Letters, v. 130, no. 1-4, p. 127-139.
- Halls, H.C., Davis, D.W., Stott, G.M., Ernst, R.E., and Hamilton, M.A., 2008, The Paleoproterozoic Marathon Large Igneous Province: New evidence for a 2.1 Ga long-lived mantle plume event along the southern margin of the North American Superior Province: Precambrian Research, v. 162, no. 3-4, p. 327-353.
- Halls, H.C., and Davis, D.W., 2004, Paleomagnetism and U-Pb geochronology of the 2.17 Ga Biscotasing dyke swarm, Ontario, Canada: Evidence for vertical-axis crustal rotation across the Kapuskasing Zone: Canadian Journal of Earth Sciences, v. 41, p. 255-269.
- Halls, H. C., and Heaman, L. M., 2000, The paleomagnetic significance of new U–Pb age data from the Molson dyke swarm, Cauchon Lake area, Manitoba: Canadian Journal of Earth Sciences, v. 37, no. 6, p. 957-966.
- Hamilton, M., Buchan, K., Ernst, R., and Scott, G., Widespread and Short-Lived 1870 Ma Mafic Magmatism Along the Northern Superior Craton Margin, *in* Proceedings American Geophysical Union-Geological Association of Canada, Joint Meeting (abstract# GA11A-01) 2009.

- Heimlich, R. A., Nelson, G. C., and Gallagher, G. L., 1973, Metamorphosed mafic dikes from the southern Bighorn Mountains, Wyoming: Geological Society of America Bulletin, v. 84, p. 1439-1450.
- Hinrichs, E. N., Kent, B. H., and Pierce, F. W., 1990, Bedrock geologic map and coal sections in the Buffal 30' x 60' Quadrangle, Johnson and Campbell counties, Wyoming: USGS Miscellaneous Investigations Series I-1923-A.
- Hoy, R. G., and Ridgway, K. D., 1997, Structural and sedimentological development of footwall growth synclines along an intraforeland uplift, east-central Bighorn Mountains, Wyoming: Geological Society of America Bulletin, v. 109, no. 8, p. 915-935.
- Irving, E., Baker, J., Hamilton, M., and Wynne, P. J., 2004, Early Proterozoic geomagnetic field in western Laurentia: implications for paleolatitudes, local rotations and stratigraphy: Precambrian Research, v. 129, no. 3-4, p. 251-270.
- Irving, E., and McGlynn, J. C., 1979, Paleomagnetism in the Coronation Geosyncline and arrangement of continents in the middle Proterozoic: Geophys. J. R. astr. Soc., v. 58, p. 309-336.
- Irving, E., Park, J. K., and McGlynn, J. C., 1972, Paleomagnetism of the Et-Then Group and Mackenzie Diabase in the Great Slave Lake Area: Canadian Journal of Earth Sciences, v. 9, no. 6, p. 744-755.
- Jones, C. H., 2002, User-driven integrated software lives: "Paleomag" paleomagnetism analysis on the Macintosh: Computers and Geosciences, v. 28, p. 1145-1151.
- Kilian, T.M., Bleeker, W., Chamberlain, K., Evans, D.A.D., and Cousens, B., 2015, Palaeomagnetism, geochronology and geochemistry of the Palaeoproterozoic

Rabbit Creek and Powder River dyke swarms: implications for Wyoming in supercraton Superia: Geological Society, London, Special Publications, v. 424.

Kirschvink, J. L., 1980, The least-squares line and plane and the analysis of palaeomagnetic data: *Geophysical Journal International*, v. 62, no. 3, p. 699-718.

Kirschvink, J. L., Kopp, R. E., Raub, T. D., Baumgartner, C. T., and Holt, J. W., 2008, Rapid, precise, and high-sensitivity acquisition of paleomagnetic and rock-magnetic data: Development of a low-noise automatic sample changing system for superconducting rock magnetometers: *Geochem. Geophys. Geosyst.*, v. 9, no. 5, p. Q05Y01.

Krogh, T.E., 1973, A low-contamination method for hydrothermal decomposition of zircon and extraction of U and Pb for isotopic age determinations: *Geochimica et Cosmochimica Acta*, v. 37, p. 485-494.

Lopez, D. A., 2001, Preliminary geologic map of the Red Lodge 30' x 60' quadrangle, South-Central Montana: Montana Bureau of Mines and Geology Open File No 423.

Ludwig, K.R., 1988, PBDAT for MS-DOS, a computer program for IBM-PC compatibles for processing raw Pb-U-Th isotope data, version 1.24: U.S. Geological Survey, Open-File Report 88-542, 32 pp.

Ludwig, K.R., 1991, ISOPLOT for MS-DOS, a plotting and regression program for radiogenic-isotope data, for IBM-PC compatible computers, version 2.75: U.S. Geological Survey, Open-File Report 91-445, 45 pp.

McCombs, J. A., Dahl, P. S., and Hamilton, M. A., 2004, U-Pb ages of Neoproterozoic granitoids from the Black Hills, South Dakota, USA: implications for crustal

evolution in the Archean Wyoming province: *Precambrian Research*, v. 130, no. 1, p. 161-184.

McGlynn, J. C., Hanson, G. N., Irving, E., and Park, J. K., 1974, Paleomagnetism and Age of Nonacho Group Sandstones and Associated Sparrow Dikes, District of Mackenzie: *Canadian Journal of Earth Sciences*, v. 11, no. 1, p. 30-42.

McGlynn, J. C., and Irving, E., 1978, Multicomponent magnetization of the Pearson Formation (Great Slave Supergroup, N.W.T.) and the Coronation loop: *Canadian Journal of Earth Sciences*, v. 15, no. 4, p. 642-654.

Mitchell, R. N., Hoffman, P. F., and Evans, D. A. D., 2010, Coronation loop resurrected: Oscillatory apparent polar wander of Orosirian (2.05-1.8 Ga) paleomagnetic poles from Slave craton: *Precambrian Research*, v. 179, no. 1-4, p. 121-134.

Mueller, P. A., Foster, D. A., Mogk, D. W., and Wooden, J. L., 2004, New insights into the Proterozoic evolution of the western margin of Laurentia and their tectonic implications: *Geological Society of America Abstracts with Programs*, v. 36, no. 404.

Mueller, P. A., Wooden, J. L., Mogk, D. W., and Foster, D. A., 2011, Paleoproterozoic evolution of the Farmington zone: Implications for terrane accretion in southwestern Laurentia: *Lithosphere*, v. 3, no. 6, p. 401-408.

Nabelek, P. I., Liu, M., and Sirbescu, M. L., 2001, Thermo-rheological, shear heating model for leucogranite generation, metamorphism, and deformation during the Proterozoic Trans-Hudson orogeny, Black Hills, South Dakota: *Tectonophysics*, v. 342, no. 3, p. 371-388.

- Nelson, S. T., Harris, R. A., Dorais, M. J., Heizler, M., Constenius, K. N., and Barnett, D. E., 2002, Basement complexes in the Wasatch fault, Utah, provide new limits on crustal accretion: *Geology*, v. 30, no. 9, p. 831-834.
- Osterwald, F. W., 1978, Structure and petrology of the northern Big Horn Mountains, Wyoming: *The Geological Survey of Wyoming, Bulletin*, v. 48, p. 1-47.
- Park, J. K., Irving, E., and Donaldson, J. A., 1973, Paleomagnetism of the Precambrian Dubawnt Group: *Geological Society of America Bulletin*, v. 84, no. 3, p. 859-870.
- Parrish, R.R., Roddick, J.C., Loveridge, W.D., and Sullivan, R.D., 1987, Uranium-lead analytical techniques at the geochronology laboratory, Geological Survey of Canada, in *Radiogenic age and isotopic studies, Report 1: Geological Survey of Canada Paper 87-2*, p. 3-7.
- Prinz, M., 1964, Geologic Evolution of the Beartooth Mountains, Montana and Wyoming. Part 5. Mafic Dike Swarms of the Southern Beartooth Mountains: *Geological Society of America Bulletin*, v. 75, no. 12, p. 1217-1248.
- Rainbird, R. H., and Davis, W. J., 2007, U-Pb detrital zircon geochronology and provenance of the late Paleoproterozoic Dubawnt Supergroup: Linking sedimentation with tectonic reworking of the western Churchill Province, Canada: *Geological Society of America Bulletin*, v. 119, no. 3-4, p. 314-328.
- Redden, J. A., and DeWitt, E., 1996, Early Proterozoic tectonic history of the Black Hills - An atypical Trans-Hudson orogen: *Geological Society of America Abstracts with Programs*, v. 28, no. 7, p. A-315.
- Reid, A. B., McMurry, E. W., and Evans, M. E., 1981, Paleomagnetism of the Great Slave Supergroup, Northwest Territories, Canada: multicomponent magnetization

of the Kahochella Group: *Canadian Journal of Earth Sciences*, v. 18, no. 3, p. 574-583.

Rioux, M., Bowring, S., Dudás, F., Hanson, R., 2010, Characterizing the U-Pb systematics of baddeleyite through chemical abrasion: application of multi-step digestion methods to baddeleyite geochronology. *Contrib Mineral Petrol* DOI 10.1007/s00410-010-0507-1

Ross, M. E., and Heimlich, R. A., 1972, Petrology of Precambrian mafic dikes from the Bald Mountain area, Bighorn Mountains, Wyoming: *Geological Society of America Bulletin*, v. 83, p. 1117-1124.

Schmidt, P. W., 1980, Paleomagnetism of igneous rocks from the Belcher Islands, Northwest Territories, Canada: *Canadian Journal of Earth Sciences*, v. 17, no. 7, p. 807-822.

Söderlund, U., and Johansson, L., 2002, A simple way to extract baddeleyite (ZrO₂): *Geochemistry, Geophysics, Geosystems*, v. 3, no. 2, p. 1–7.

Sullivan, W. A., and Beane, R. J., 2013, A new view of an old suture zone: Evidence for sinistral transpression in the Cheyenne belt: *Geological Society of America Bulletin*.

Stacey, J.S. and Kramers, J.D., 1975, Approximation of terrestrial lead isotope evolution by a two-stage model: *Earth and Planetary Science Letters*, v. 26, p. 207-221.

Steiger, R.H. and Jäger, E., 1977, Subcommittee on geochronology: convention on the use of decay constants in geo- and cosmochronology: *Earth and Planetary Science Letters*, v. 36, p. 359-362.

- Weber, W., 1990, The Churchill–Superior boundary zone, southeast margin of the Trans-Hudson orogen: a review: The Early Proterozoic Trans-Hudson Orogen of North America. Edited by JF Lewry and MR Stauffer. Geological Association of Canada Special Paper, v. 37, p. 41-55.
- Whitmeyer, S. J., and Karlstrom, K. E., 2007, Tectonic model for the Proterozoic growth of North America: *Geosphere*, v. 3, no. 4, p. 220-259.
- Worthington, L.L., Miller, K.C., Erslev, E.A., Anderson, M.L., Chamberlain, K.R., Sheehan, A.F., Yeck, W.L., Harder, S.H., and Siddoway, C.S., 2016, Crustal structure of the Bighorn Mountains region: Precambrian influence on Laramide shortening and uplift in north-central Wyoming: *Tectonics*, v. 35, p. 208–236, doi:10.1002/2015TC003840.
- Zhai, Y., Halls, H. C., and Bates, M. P., 1994, Multiple episodes of dike emplacement along the northwestern margin of the Superior Province, Manitoba: *J. Geophys. Res.*, v. 99, no. B11, p. 21717-21732.